Bimetallic Nanoparticles in Supported Ionic Liquid Phases as Multifunctional Catalysts for the Selective Hydrodeoxygenation of Aromatic Substrates

Lisa Offner-Marko, Alexis Bordet, Gilles Moos, Simon Tricard, Simon Rengshausen, Bruno Chaudret, Kylie L. Luska, and Walter Leitner

Abstract: *Bimetallic iron–ruthenium nanoparticles embedded in an acidic supported ionic liquid phase (FeRu@SILP+IL-SO$_3$H) act as multifunctional catalysts for the selective hydrodeoxygenation of carbonyl groups in aromatic substrates. The catalyst material is assembled systematically from molecular components to combine the acid and metal sites that allow hydrogenolysis of the C=O bonds without hydrogenation of the aromatic ring. The resulting materials possess high activity and stability for the catalytic hydrodeoxygenation of C=O groups to CH$_2$ units in a variety of substituted aromatic ketones and, hence, provide an effective and benign alternative to traditional Clemmensen and Wolff–Kishner reductions, which require stoichiometric reagents. The molecular design of the FeRu@SILP+IL-SO$_3$H materials opens a general approach to multifunctional catalytic systems (MM'@SILP+IL-func).*

The catalytic hydrodeoxygenation of carbonyl groups to methylene units in the side chains of aromatic substrates has attracted considerable attention for the production of alkyl-substituted aromatic structures in commodity and fine chemicals.[1] It is also considered an important enabler for the deoxygenation of building blocks from lignocellulosic biomass towards value-added chemicals and tailor-made fuels.[2a–f] However, the large-scale synthetic application of this transformation has been hindered by the lack of suitable catalysts that allow for selective catalytic hydrodeoxygenation
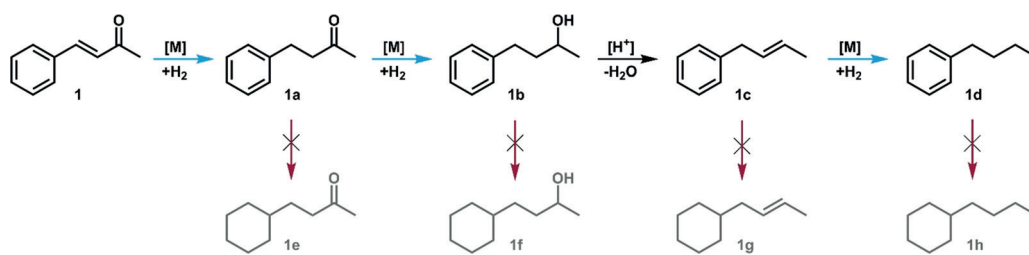
[*] M. Sc. L. Offner-Marko, Dr. A. Bordet, M. Sc. G. Moos,
M. Sc. S. Rengshausen, Dr. K. L. Luska, Prof. Dr. W. Leitner
Institut für Technische und Makromolekulare Chemie
RWTH Aachen University
Worringerweg 2, 52074 Aachen (Germany)
E-mail: walter.leitner@cec.mpg.de

M. Sc. L. Offner-Marko, Dr. A. Bordet, M. Sc. G. Moos,
M. Sc. S. Rengshausen, Prof. Dr. W. Leitner
Max-Planck-Institut für Chemische Energiekonversion
45470 Mülheim an der Ruhr (Germany)

Dr. A. Bordet, Dr. S. Tricard, Prof. Dr. B. Chaudret
Laboratoire de Physique et Chimie de Nano-Objets
Université de Toulouse, INSA, UPS, LPCNO, CNRS-UMR5215
135 Avenue de Rangueil, 31077 Toulouse (France)

Supporting information and the ORCID identification number(s) for the author(s) of this article can be found under:
https://doi.org/10.1002/anie.201806638.

Scheme 1. Selective catalytic hydrodeoxygenation of aromatic carbonyl compounds as a possible route to alkyl-substituted aromatics, opening new synthetic pathways, for example, from Friedel–Crafts acylation products or lignin derivatives.

of aromatic ketones without concomitant hydrogenation of the aromatic ring (Scheme 1).[3] Stoichiometric methods such as the Clemmensen[4] and Wolff–Kishner[5] reductions often remain the methods of choice for the removal of carbonyl moieties from aromatic substrates, despite the fact that they rely on the use of toxic reagents and/or create large amounts of undesired and problematic waste.[1] Current synthetic pathways involving the hydrodeoxygenation of aromatic substrates cannot fulfill the requirements of high yields, selectivity, stability, productivity, safety, and environmental compatibility.[6] Consequently, recent efforts have been devoted to the development of selective hydrodeoxygenation catalysts, typically based on conventional materials for heterogeneous catalysis.[7a–j] While promising results have been obtained in some cases for individual substrates, most of the traditional solid catalysts show severe limitations such as low hydrogenation selectivity,[8a–c] restriction to only benzylic carbonyl groups,[7a–c] low stability,[7d–e] formation of side-products,[7f] or high catalyst loadings approaching almost stoichiometric amounts of the active metal component.[7g]

In the present paper, we describe the design, preparation, and application of novel bifunctional catalysts for the selective hydrodeoxygenation of aromatic substrates using a molecular approach to assemble the key components of the active materials.

The design of the catalyst was based on the analysis of the desired sequence of bond-breaking and bond-forming events to achieve the overall transformation, exemplified for benzylideneacetone (**1**) as a prototypical substrate in Scheme 2. The metal-catalyzed hydrogenation of the C=C and C=O bond leads to the corresponding alcohol **1b**. Then, the C—O bond is broken through an acid-catalyzed E1- or E2-type mechanism, resulting in a carbocation or olefin intermediate (only the

Scheme 2. The complex reaction network to be controlled for selective deoxygenation of aromatic substrates, exemplified for benzylideneacetone (**1**).

latter is shown for clarity in Scheme 2). A second metal-catalyzed hydrogenation leads to butylbenzene (**1d**) as the desired product. The catalytic hydrogenation of the aromatic ring must be strictly avoided at each stage. Thus, the challenge for catalyst design was to combine a highly selective metal component for hydrogenation with a sufficiently acidic functionality to facilitate the C−O bond cleavage.

A recently emerging approach to prepare multifunctional catalytic systems is based on well-defined metal nanoparticles (NPs) synthesized from organometallic precursors that are embedded in ionic liquid (IL) matrices.[9a–g] Herein, we present a version of such materials that combines covalently grafted non-functionalized IL-type structures with physisorbed functionalized ILs on silica as support (supported ionic liquid phases, SILPs). This approach allows the controlled formation of NPs on the non-functionalized SILP and provides a large degree of freedom for post-modification with the functionalized IL. The resulting materials are denoted as MM′@SILP + IL-func, in which MM′ defines the metal(s), SILP the covalently grafted IL, and IL-func the physisorbed IL (e.g., IL-SO$_3$H for the acidic IL used in this study).[10a–e]

To address the present synthetic challenge, the combination of bimetallic iron–ruthenium nanoparticles (FeRu NPs) with an acidic support appeared very promising. Recently, Fe$_{25}$Ru$_{75}$ NPs immobilized on a non-functionalized SILP (Fe$_{25}$Ru$_{75}$@SILP) were shown to exhibit high activity for the reduction of C=C, C=O, and C=N groups in substituted aromatic substrates, while preventing the reduction of aromatic moieties.[11] Another recent study also outlined a synergistic effect in bimetallic FeRu@SILP catalysts used for the hydrogenation of CO$_2$ to hydrocarbons.[12] However, attempts to synthesize Fe$_{25}$Ru$_{75}$ NPs on supports in which the acid functions are covalently grafted prior to NP formation (SILP-SO$_3$H)[9e–g] proved unsuccessful owing to the unfavorable interaction of the Fe-precursor with the acid functionality. The hydrodeoxygenation of **1** with the resulting materials only led to the hydrogenation intermediates **1a**, **1b**, **1e**, and **1f** without exhibiting any deoxygenation activity (see the Supporting Information, Tables S1 and S3 and Figure S1). Preparing Fe$_{25}$Ru$_{75}$ NPs on a non-functionalized SILP and carrying out the transformation in the presence of *p*-toluenesulfonic acid (*p*-TsOH) as acidic additive yielded significant amounts of the desired product **1d**, albeit with only low selectivity (**1a**:**1b**:**1d** = 36:31:32). Finally, excellent activity and selectivity were obtained using a sulfonic acid-functionalized imidazolium IL, [BSO$_3$BIM][NTf$_2$] (IL-

SO$_3$H), as acid additive. **1d** was detected by GC essentially as the sole product in the reaction mixture with greater than 99% yield at full conversion of **1** upon using 2.50 equivalents of IL-SO$_3$H with regard to the total metal loading (4 mol% relative to **1**) within 16 h at 150°C under H$_2$ (50 bar at RT) (Table S4). Based on these promising results, the controlled preparation of the Fe$_{25}$Ru$_{75}$@SILP + IL-SO$_3$H material sketched in Figure 1 was targeted to ensure an intimate contact between the NPs and the acid moieties in

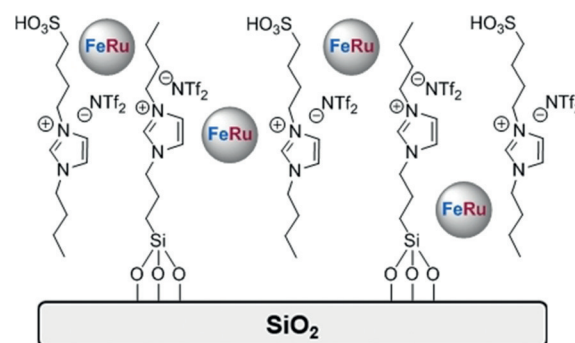**Figure 1.** Schematic of iron–ruthenium nanoparticles immobilized on a sulfonic acid-functionalized supported ionic liquid phase (Fe$_{25}$Ru$_{75}$@SILP + IL-SO$_3$H) as a bifunctional catalyst for the hydrodeoxygenation of carbonyl-substituted aromatic substrates.

the bifunctional catalyst. The synthesis of Fe$_{25}$Ru$_{75}$ NPs immobilized on a non-functionalized SILP was accomplished using a reported procedure.[11] In brief, the NPs were prepared through the in situ reduction of a mesitylene solution of {Fe[N(Si(CH$_3$)$_3$)$_2$]$_2$}$_2$ and [Ru(cod)(cot)] in the presence of the SILP material under an atmosphere of H$_2$ (3 bar) at 150°C. The oxidation state and alloy extent of the Fe$_{25}$Ru$_{75}$ NPs in Fe$_{25}$Ru$_{75}$@SILP were previously studied by XANES and EXAFS, evidencing zerovalent Fe and Ru atoms organized in a homophilic bimetallic structure (bimetallic phase with more Fe and Ru homoatomic interactions than in a perfect bimetallic structure).[11] The physisorption of IL-SO$_3$H onto Fe$_{25}$Ru$_{75}$@SILP to prepare the bifunctional catalyst (Fe$_{25}$Ru$_{75}$@SILP + IL-SO$_3$H) was achieved by stirring a suspension of Fe$_{25}$Ru$_{75}$@SILP and IL-SO$_3$H in acetone at RT.

As expected, the surface area and the pore volume were significantly reduced upon physisorption of the IL-SO$_3$H on Fe$_{25}$Ru$_{75}$@SILP according to BET analysis. These data are in good agreement with a pore-filling degree (or α factor) of 0.7. Detailed analysis by TEM showed that the size of the metal nanoparticles (2.9 nm) did not change significantly upon physisorption; however, the NPs were less homogeneously dispersed across the support than before. STEM/EDS elemental mapping evidenced a clear correlation between sulfur

© 2018 The Authors. Published by Wiley-VCH Verlag GmbH & Co. KGaA, Weinheim

and metal concentration, with higher sulfur content (ca. 2-fold) in zones containing NPs as compared to zones without NPs. This observation indicates a preference of the NPs to accumulate in areas with large amounts of physisorbed IL-SO$_3$H. STEM/EDS elemental mapping and SEM/EDS demonstrated that, despite this noticeable redistribution, the NPs still contain both Fe and Ru (Figure 2) in an unaffected metal ratio (see the Supporting Information, Table S2 and Figures S2, S3, and S5, for complete characterization details).
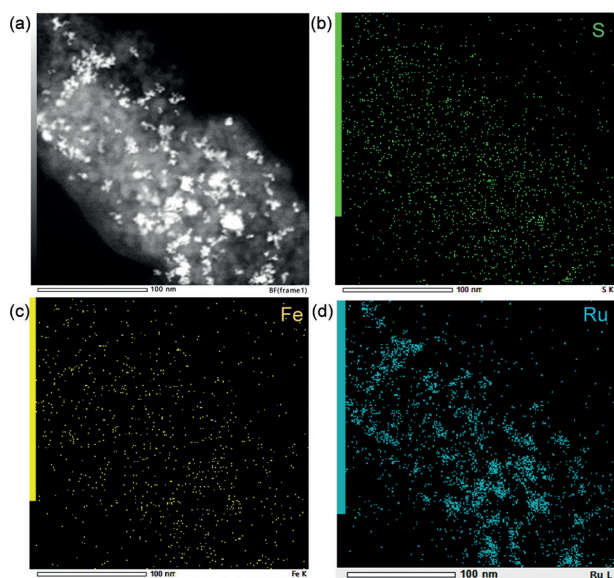

Figure 2. Scanning transmission electron microscopy with energy dispersive X-ray spectroscopy (STEM/EDS) elemental mappings of Fe$_{25}$Ru$_{75}$@SILP+IL-SO$_3$H. a) STEM-HAADF image of Fe$_{25}$Ru$_{75}$@SILP+IL-SO$_3$H, b) S, c) Fe, and d) Ru.

These results indicate that the physisorption of the acidic ionic liquid onto Fe$_{25}$Ru$_{75}$@SILP did not affect the integrity of the Fe$_{25}$Ru$_{75}$ NPs (size, metal ratio). These data substantiate the conclusion that Fe$_{25}$Ru$_{75}$ NPs retain their oxidation state and alloy structure after physisorption of the acidic ionic liquid and consist of zerovalent Fe and Ru atoms organized in a homophilic bimetallic structure.

The reaction profile for the hydrodeoxygenation of benzylideneacetone (**1**) catalyzed by Fe$_{25}$Ru$_{75}$@SILP+IL-SO$_3$H is shown in Figure 3. A mixture of hydrogenation intermediates **1a** and **1b** (58%) and the deoxygenation product **1d** (42%) was formed already after 1 h. As the reaction progressed, the hydrogenation intermediates, **1a** and **1b**, were gradually consumed and an almost quantitative yield of **1d** was obtained after 12 h. During the entire reaction sequence, no species resulting from the hydrogenation of the aromatic moiety were observed.

The close vicinity of the IL-SO$_3$H with the bimetallic particles as evidenced by the STEM/EDS data appears to be crucial for efficient hydrogenolysis. In contrast to Fe$_{25}$Ru$_{75}$@SILP+IL-SO$_3$H, a physical mixture of non-functionalized Fe$_{25}$Ru$_{75}$@SILP and metal-free SILP-SO$_3$H resulted in only slow formation of **1d** (7%) with **1a** (70%) and **1b** (18%) being the main products after 16 h under
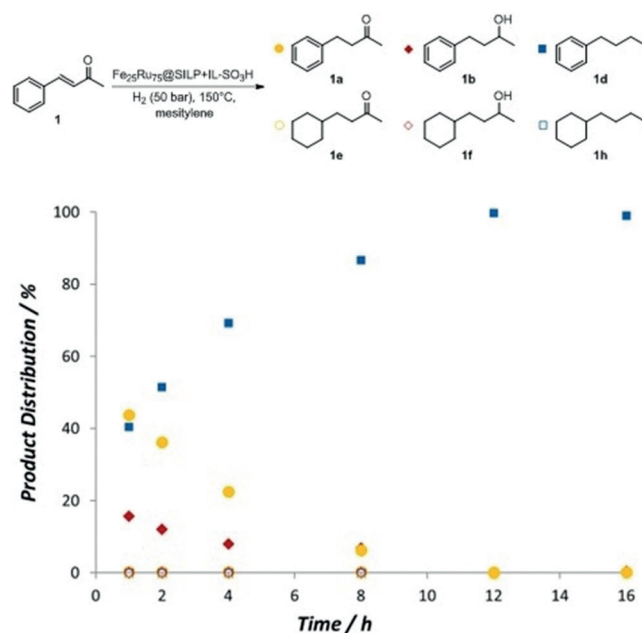

Figure 3. Reaction profile for the hydrodeoxygenation of benzylideneacetone (**1**) using Fe$_{25}$Ru$_{75}$@SILP+IL-SO$_3$H. Reaction conditions: Fe$_{25}$Ru$_{75}$@SILP+IL-SO$_3$H (58 mg of catalyst containing 0.015 mmol total metal and 0.038 mmol (2.50 equiv.) IL-SO$_3$H), substrate (0.38 mmol), mesitylene (0.5 mL), H$_2$ (50 bar), 150°C. Conversion and product distribution were determined by GC using tetradecane as an internal standard.

identical reaction conditions (see the Supporting Information, Table S4). Similar synergistic effects were observed for Ru$_{100}$@SILP-SO$_3$H in the deep hydrodeoxygenation of phenols.[9f] With leaching of physisorbed ionic liquids being a well-known issue in solution phase catalysis,[13a,b] the stability of Fe$_{25}$Ru$_{75}$@SILP+IL-SO$_3$H was carefully studied. Conversion and selectivity towards the formation of butylbenzene (**1d**) were constant upon recycling of the catalyst material for at least four times without any make-up or regeneration (see the Supporting Information, Table S5). This is in good agreement with quantitative SEM/EDS analysis, which did not evidence significant leaching of the metals nor of the acidic ionic liquid under reaction conditions. TEM analysis showed no NP growth or aggregation, and the conservation of their bimetallic nature was confirmed by STEM/EDS elemental mapping. BET analysis indicated that the textural properties of the bifunctional catalyst did not change (see the Supporting Information, Table S2 and Figures S2–6, for complete characterization details). The excellent stability of the catalyst is most likely reflecting favorable interactions between the covalently grafted and physisorbed ionic liquid structures arising from their molecular similarity.

The substrate scope for the selective hydrodeoxygenation using the bifunctional Fe$_{25}$Ru$_{75}$@SILP+IL-SO$_3$H catalyst was assessed with a range of carbonyl-substituted aromatic substrates (Table 1 and Table S7). Interestingly, while benzylideneacetone (**1**) was converted to the deoxygenation product **1d** in quantitative yields at 150°C (Table 1, Entry 1), the efficient hydrodeoxygenation of 1-phenyl-1-

Table 1: Hydrodeoxygenation of carbonyl-substituted aromatic substrates using Fe$_{25}$Ru$_{75}$@SILP+IL-SO$_3$H.[a]

Entry	Substrate	Product [%][b]
1	**1**	**1d** > 99[c]
2	**1a**	**1d** > 99[c]
3	**2**	**1d** 94
4	**3**	**1d** 82[d]
5	**4**	**4a** 91
6	**5**	**5a** 92
7	**6**	**6a** 95
8	**7**	**7a** > 99
9	**8**	**8a** > 99

[a] Reaction conditions: Fe$_{25}$Ru$_{75}$@SILP+IL-SO$_3$H (58 mg catalyst containing 0.015 mmol total metal and 0.038 mmol (2.50 equiv.) IL-SO$_3$H), substrate (0.38 mmol, 25 equiv.), mesitylene (0.5 mL). [b] Yield determined by GC, conversion > 99%. [c] 150°C. Remainders of reaction mixtures were composed of dimeric by-products or [d] **4a** (12%) and dimeric by-products (6%).

butanone (**2**) to give the same product **1d** required a temperature of 175°C (Table 1, Entry 2). The hydrodeoxygenation of the 1,3-diketone (**3**) at 175°C also proceeded smoothly to give high yields of **1d** (Table 1, Entry 3). Performing this reaction at 100°C evidenced the presence of **2** (22%) and 4-phenyl-2-butanone (**1a**) (8%) as intermediates (see the Supporting Information, Table S9). 4-phenyl-2-butene (**1c**) was also observed as an intermediate of the reaction at 100°C

(Table S9), which supports the reaction pathway discussed in Scheme 2. The greater amount of intermediate **2** as compared to **1a** indicates that the deoxygenation of the non-benzylic ketone is favored over the benzylic ketone. This was confirmed by comparative rate studies for the hydrodeoxygenation of **2** and **1a**, demonstrating a two-fold higher reaction rate for **1a** (Figure 4 and Figure S8). This unique reactivity pattern is in sharp contrast to previously reported hydrodeoxygenation catalysts.
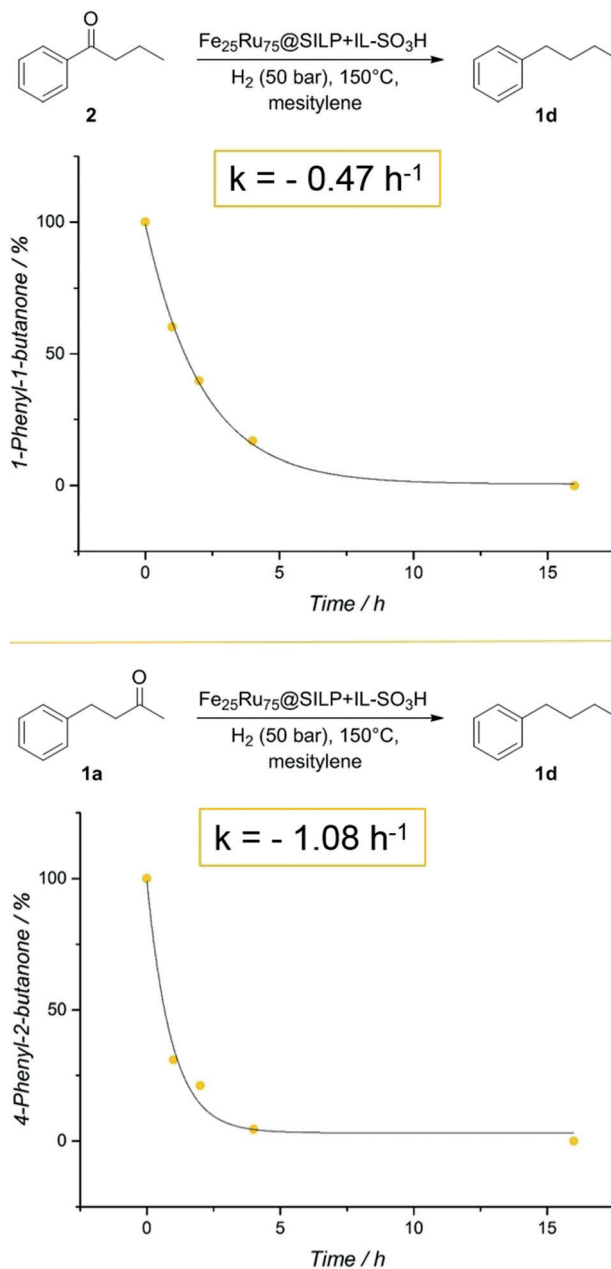

$k = - 0.47 \ h^{-1}$

$k = - 1.08 \ h^{-1}$

Figure 4. Comparative rate studies for the hydrodeoxygenation of 1-phenyl-1-butanone (**2**) and 4-phenyl-2-butanone (**1a**) using Fe$_{25}$Ru$_{75}$@SILP+IL-SO$_3$H. Reaction conditions: Fe$_{25}$Ru$_{75}$@SILP+IL-SO$_3$H (58 mg catalyst containing 0.015 mmol total metal and 0.038 mmol (2.50 equiv.) IL-SO$_3$H), substrate (0.38 mmol), mesitylene (0.5 mL), H$_2$ (50 bar), 150°C. Conversion was determined by GC using tetradecane as an internal standard.

The hydrodeoxygenation of Friedel–Craft acylation products such as **2** provides an interesting alternative to classical Friedel–Crafts alkylation reactions, which are prone to over-alkylation and carbocation rearrangements. The $Fe_{25}Ru_{75}@SILP + IL-SO_3H$ catalyst proved to be very versatile in this context. The hydrodeoxygenation of acetophenone (**4**) and its derivatives **5** and **6** gave the corresponding deoxygenation products in over 90 % yield, irrespective of the presence of electron-donating (**5**) or electron-withdrawing (**6**) groups in the *para*-position. Acylated naphthalene (**7**) was converted to 2-ethylnapthalene (**7a**) in quantitative yields under standard reaction conditions. Notably, the conversion of diphenylketone (**8**) to diphenylmethane (**8a**) was also quantitative, indicating that the formation of an olefinic intermediate is not required in case sufficiently stable carbocations can be formed.

Using $Fe_{25}Ru_{75}@SILP + IL-SO_3H$, the hydrogenation of aromatic moieties was not observed for any of the substrates, even at prolonged reaction time. In sharp contrast, the use of monometallic $Ru_{100}@SILP + IL-SO_3H$ catalysts under similar reaction conditions led to deep hydrogenation of all substrates, yielding completely saturated deoxygenation products or product mixtures (for detailed results, see the Supporting Information, Table S8). Monometallic $Fe_{100}@SILP$ catalysts were previously tested and found inactive for the reduction of C=O bonds.[11] This emphasizes how the bimetallic FeRu@SILP + IL-SO_3H catalyst provides a highly selective route towards the synthesis of a wide range of aromatic deoxygenation products that are not accessible using standard catalytic systems.

As a general conclusion, the combination of ionic liquid (IL)-modified surfaces and nanoparticle (NP) synthesis from organometallic precursors provides a highly flexible and versatile molecular approach to control the metal as well as the acid component of multifunctional catalytic systems. Covalent grafting and physisorption of the ILs allows separation of the functionalization from the stabilization effect of the SILP. This largely extends the range of possible metal precursor complexes as demonstrated in this study for the acid sensitive iron sources, opening a huge parameter space for multi-metallic NPs to be assembled on the SILP surface. The post-synthesis modification through the physisorption of functionalized ILs ensures an intimate contact between the desired functionality and the metal components. The potential of this approach for designing and generating multifunctional catalytic systems with tailor-made reactivity for challenging catalytic transformations is exemplified with the $Fe_{25}Ru_{75}@SILP + IL-SO_3H$ material for the selective hydrodeoxygenation of aromatic ketones. Thus, the presented multifunctional catalytic system constitutes an interesting alternative to Clemmensen and Wolff–Kishner reductions, opening a greener approach to alkylated aromatic compounds.

Acknowledgements

Conflict of interest

The authors declare no conflict of interest.

[1] R. O. Hutchins, M. K. Hutchins in *Comprehensive Organic Synthesis, Vol. 8* (Ed.: I. Fleming), Elsevier, Oxford, **1991**, pp. 327–362.

[2] a) A. Corma, S. Iborra, A. Velty, *Chem. Rev.* **2007**, *107*, 2411–2502; b) A. M. Ruppert, K. Weinberg, R. Palkovits, *Angew. Chem. Int. Ed.* **2012**, *51*, 2564–2601; *Angew. Chem.* **2012**, *124*, 2614–2654; c) M. Besson, P. Gallezot, C. Pinel, *Chem. Rev.* **2014**, *114*, 1827–1870; d) T. vom Stein, J. Klankermayer, W. Leitner in *Catalysis for the Conversion of Biomass and Its Derivatives* (Eds: M. Behrens, A. K. Datye), epubli, Berlin, **2013**, pp. 411–434; e) K. L. Luska, P. Migowski, W. Leitner, *Green Chem.* **2015**, *17*, 3195–3206; f) W. Leitner, J. Klankermayer, S. Pischinger, H. Pitsch, K. Kohse-Höinghaus, *Angew. Chem. Int. Ed.* **2017**, *56*, 5412–5452; *Angew. Chem.* **2017**, *129*, 5500–5544.

[3] J. Magano, J. R. Dunetz, *Org. Process Res. Dev.* **2012**, *16*, 1156–1184.

[4] E. Vedejs, *Org. React.* **1975**, *22*, 401–422.

[5] D. Todd, *Org. React.* **1948**, *4*, 378–422.

[6] K. Hattori, H. Sajiki, K. Hirota, *Tetrahedron* **2001**, *57*, 4817–4824.

[7] a) C. Van Doorslaer, J. Wahlen, P. G. N. Mertens, B. Thijs, P. Nockemann, K. Binnemans, D. E. de Vos, *ChemSusChem* **2008**, *1*, 997–1005; b) X. J. Kong, L. G. Chen, *Catal. Commun.* **2014**, *57*, 45–49; c) L. Petitjean, R. Gagne, E. S. Beach, D. Xiao, P. T. Anastas, *Green Chem.* **2016**, *18*, 150–156; d) M. Li, J. Deng, Y. Lan, Y. Wang, *ChemistrySelect* **2017**, *2*, 8486–8492; e) C. González, P. Marín, F. V. Díez, S. Ordóñez, *Ind. Eng. Chem. Res.* **2016**, *55*, 2319–2327; f) V. Kogan, Z. Aizenshtat, R. Neumann, *Angew. Chem. Int. Ed.* **1999**, *38*, 3331–3334; *Angew. Chem.* **1999**, *111*, 3551–3554; g) F. Zaccheria, N. Ravasio, M. Ercoli, P. Allegrini, *Tetrahedron Lett.* **2005**, *46*, 7743–7745; h) M. Bejblová, P. Zámostný, L. Červený, J. Čejka, *Appl. Catal. A* **2005**, *296*, 169–175; i) D. Procházková, P. Zámostný, M. Bejblová, L. Červený, J. Čejka, *Appl. Catal. A* **2007**, *332*, 56–64; j) J. Ma, S. Liu, X. Kong, X. Fan, X. Yan, L. Chen, *Res. Chem. Intermed.* **2012**, *38*, 1341–1349.

[8] a) P. N. Rylander in *Hydrogenation Methods*, Academic Press, New York, **1985**, pp. 66–77; b) S. Nishimura in *Handbook of Heterogeneous Catalytic Hydrogenation for Organic Synthesis*,

Wiley-VCH, New York, **2001**, pp. 170–225; c) A. Stanislaus, B. H. Cooper, *Catal. Rev. Sci. Eng.* **1994**, *36*, 75–123.

[9] a) N. Yan, Y. Yuan, R. Dykeman, Y. Kou, P. J. Dyson, *Angew. Chem. Int. Ed.* **2010**, *49*, 5549–5553; *Angew. Chem.* **2010**, *122*, 5681–5685; b) Y. Zhu, Z. N. Kong, L. P. Stubbs, H. Lin, S. Shen, E. V. Anslyn, J. A. Maguire, *ChemSusChem* **2010**, *3*, 67–70; c) S. Winterle, M. A. Liauw, *Chem. Ing. Tech.* **2010**, *82*, 1211–1214; d) J. Julis, W. Leitner, *Angew. Chem. Int. Ed.* **2012**, *51*, 8615–8619; *Angew. Chem.* **2012**, *124*, 8743–8747; e) K. L. Luska, J. Julis, E. Stavitski, D. N. Zakharov, A. Adams, W. Leitner, *Chem. Sci.* **2014**, *5*, 4895–4905; f) K. L. Luska, P. Migowski, S. El Sayed, W. Leitner, *Angew. Chem. Int. Ed.* **2015**, *54*, 15750–15755; *Angew. Chem.* **2015**, *127*, 15976–15981; g) K. L. Luska, P. Migowski, S. El Sayed, W. Leitner, *ACS Sustainable Chem. Eng.* **2016**, *4*, 6186–6192.

[10] a) R. Fehrmann, A. Riisager, M. Haumann in *Supported Ionic Liquids: Fundamentals and Applications*, Wiley-VCH, Weinheim, **2014**; b) A. Riisager, P. Wasserscheid, R. van Hal, R.

Fehrmann, *J. Catal.* **2003**, *219*, 452–455; c) M. H. Valkenberg, C. deCastro, W. F. Hölderich, *Green Chem.* **2002**, *4*, 88–93; d) C. P. Mehnert, R. A. Cook, N. C. Dispenziere, M. Afeworki, *J. Am. Chem. Soc.* **2002**, *124*, 12932–12933; e) U. Kernchen, B. Etzold, W. Korth, A. Jess, *Chem. Eng. Technol.* **2007**, *30*, 985–994.

[11] K. L. Luska, A. Bordet, S. Tricard, I. Sinev, W. Grünert, B. Chaudret, W. Leitner, *ACS Catal.* **2016**, *6*, 3719–3726.

[12] M. I. Qadir, A. Weilhard, J. A. Fernandes, I. de Pedro, B. J. C. Vieira, J. C. Waerenborgh, J. Dupont, *ACS Catal.* **2018**, *8*, 1621–1627.

[13] a) P. Migowski, K. L. Luska, W. Leitner, *Nanocatalysis in Ionic Liquids*, Wiley-VCH, Weinheim, **2017**, pp. 249–273; b) P. Zhang, T. Wu, B. Han, *Adv. Mater.* **2014**, *26*, 6810–6827.